

# Structure and Binding of Alkanethiolates on Gold and Silver Surfaces: Implications for Self-Assembled Monolayers

Harrell Sellers,<sup>\*,†,‡</sup> Abraham Ulman,<sup>\*,§</sup> Yitzhak Shnidman,<sup>§</sup> and James E. Eilers<sup>§</sup>

*Contribution from the National Center for Supercomputing Applications, Beckman Institute for Advanced Science and Technology, University of Illinois, Urbana, Illinois 61801, and Corporate Research Laboratories and Computational Science Laboratory, Eastman Kodak Company, Rochester, New York, 14650-2109*

Received September 16, 1992\*

**Abstract:** We performed *ab initio* geometry optimization of HS and CH<sub>3</sub>S on cluster models of Au(111), Au(100), Ag(111), and Ag(100) surfaces, at the RECP Hartree-Fock + electron correlation (MBPT2) level. From these we determined classical force field parameters, thus opening the possibility for realistic molecular dynamics (MD) simulations of self-assembled alkanethiolate monolayers on gold and silver surfaces. We find that there are two chemisorption modes, very close in energy, for thiolates on Au(111) surfaces. In the first, the surface-S-C bond angle is ~180° (sp hybridization), while in the second it is ~104° (sp<sup>3</sup> hybridization). This suggests a possible mechanism for the annealing of alkanethiolate monolayers. We present herein the first molecular mechanics energy minimization using these new force field parameters. Self-assembled monolayers of alkanethiolates on gold and silver are different. The *ab initio* calculations presented here provide the fundamental understanding of the chemisorption of alkanethiolates on gold and silver surfaces, the surface-adsorbates bonds, and the structure of the monolayers thus formed.

## Introduction

Self-assembled monolayers (SAMs) are molecular aggregates that are spontaneously formed by the adsorption of amphifunctional molecules on a solid surface.<sup>1,2</sup> We define amphifunctional molecules as those that have one part that has strong affinity—in most cases chemical in nature—to the surface and another that has either very weak affinity or none. There are several types in SA methods that give organic monolayers. These include organosilicon on hydroxylated surfaces (SiO<sub>2</sub> on Si, Al<sub>2</sub>O<sub>3</sub> on Al, glass, etc.), alkanethiolates on gold, silver, and copper, alcohols and amines on platinum, and carboxylic acids on aluminum oxide, silver oxide, and glass.

From the energetics point of view, a self-assembling surfactant molecule consists of three parts (Figure 1). The first part is the headgroup that provides the most exothermic process, i.e., chemisorption on the substrate surface. The very strong molecular-substrate interactions result in an apparent pinning of the head group to a specific site on the surface through a chemical bond. This can be a covalent Si-O bond in the case of alkyltrichlorosilanes on hydroxylated surfaces, a covalent but slightly polar Au-S bond in the case of alkanethiolates on gold, or an ionic -CO<sub>2</sub>-Ag<sup>+</sup> bond in the case of carboxylic acids on AgO/Ag. The energies associated with the chemisorption are of the order of tens of kcal/mol, e.g., ~28 kcal/mol for thiolate on

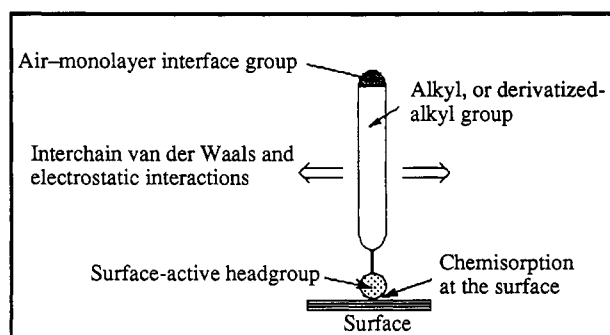


Figure 1. A schematic view of the forces in a self-assembled monolayer.

gold.<sup>3,4</sup> It is this spontaneous molecular adsorption that brings molecules close enough together and allows the short-range, dispersive, London-type, van der Waals forces to become important. The second molecular part is an organic moiety—in the most simple case an alkyl chain—and the energies associated with its interchain van der Waals interactions depend on both the chain length and the packing density and can be comparable in size to the chemisorption energy.<sup>5</sup>

Two-dimensional ordering results from intermolecular interactions such as van der Waals and electrostatic interactions.<sup>6–9</sup> In simple amphiphiles, the extent of intermolecular interactions has been suggested to be related to the spacing between the molecular head groups.<sup>10,11</sup> This spacing may be the result of the chemisorption scheme, which is determined by the nature of the adsorbate bond to the surface. For example, in self-assembled

(3) Dubois, L. H.; Zegarski, B. R.; Nuzzo, R. G. *Proc. Natl. Acad. Sci. U.S.A.* 1987, 84, 4739.

(4) Dubois, L. H.; Zegarski, B. R.; Nuzzo, R. G. *J. Am. Chem. Soc.* 1990, 112, 570.

(5) For example, we have calculated, using modified MM2 force field, van der Waals energy of -26.6 kcal/mol for a monolayer of SC<sub>16</sub>H<sub>33</sub> on Au(111).

(6) Kitagorodskii, A. I. *Organic Chemical Crystallography*; Consultants Bureau: New York, 1959; pp 177–217.

(7) Garoff, S. *Proc. Natl. Acad. Sci. U.S.A.* 1987, 84, 4729 and references cited therein.

(8) Langmuir, I. *J. Chem. Phys.* 1933, 1, 756.

(9) Epstein, H. T. *J. Colloid. Chem.* 1950, 54, 1053.

(10) Safran, S. A.; Robbins, M. O.; Garoff, S. *Phys. Rev. A* 1986, 33, 2188.

(11) Ulman, A.; Tillman, N.; Eilers, J. *Langmuir* 1989, 5, 1147.

monolayers of alkyltrichlorosilane, the Si-Si distance—determined by the Si-O-Si linkage (*d*-spacing  $1.35 \pm 0.03 \text{ \AA}$ )<sup>12</sup>—imposes molecular packing that results in minimum free volume and alkyl chains that are almost perpendicular to the surface.<sup>13</sup> The results of the work presented here show that such differences in spacing between thiol head groups do exist when thiols are chemisorbed on gold and silver surfaces.

In self-assembled monolayers, the packing and ordering are determined by the contributions of both chemisorption and intra- and interchain nonbonded (e.g., van der Waals, steric, repulsive, electrostatic) interactions. The interplay between interchain forces and the interaction with the surface, combined with entropic effects, determines both the conformation of the individual chains within the assembly and their packing and ordering with respect to each other.

The understanding of the relationships between the molecular structure of amphiphiles and their organization on different surfaces is a fundamental problem. The packing and orientation of such molecules affect the surface chemistry of the monolayer, and play an important role in phenomena of boundary lubrication, corrosion inhibition, adhesion, and catalysis.<sup>14–16</sup> Such molecular level understanding is essential for any successful molecular engineering of amphiphilic or amphifunctional molecules with useful properties. Indeed, there have been numerous attempts to explain the packing and molecular orientation in two-dimensional assemblies. These include molecular mechanics calculations of alkanethiolates on gold,<sup>11</sup> molecular dynamics simulations of alkanethiolates on gold,<sup>17</sup> of lipid membranes, and of Langmuir monolayers (molecular assemblies at the air–water interface),<sup>18–22</sup> and Brownian dynamics of Langmuir monolayers.<sup>23</sup> We content, however, that without a fundamental understanding of the chemisorption process and the surface-adsorbate bonding thus formed, modeling of self-assembled monolayers lacks a crucial component.

Chemisorption of alkanethiols on gold gives the gold(I) thiolate ( $\text{RS}^-$ ) species probably by



While the mechanism involved in the reaction of alkanethiols with gold(0) is not completely understood, it is clear now that the species chemisorbed on the gold surface is indeed a thiolate. This has been shown by X-ray photoelectron spectroscopy (XPS),<sup>24</sup> FTIR spectroscopy,<sup>25</sup> Fourier transform mass spectrometry,<sup>26</sup>

(12) Robinson, K.; Ulman, A.; Lando, J.; Mann, A. *J. Phys. Rev. Lett.*, submitted for publication.

(13) Tillman, N.; Ulman, A.; Schildkraut, J. S.; Penner, T. L. *J. Am. Chem. Soc.* **1988**, *110*, 6136.

(14) Zisman, W. A. In *Friction and Wear*; Davis, R., Ed.; Elsevier: New York, 1959; p 118.

(15) Adamson, A. W. *Physical Chemistry of Surfaces*; Wiley: New York, 1976, and references cited therein.

(16) Somorjai, G. A. *Chemistry of Two Dimensions: Surfaces*; Cornell University Press: Ithaca, NY, 1981, and references cited therein.

(17) Hautman, J.; Klein, M. L. *J. Chem. Phys.* **1989**, *91*, 4994. Hautman, J.; Bareman, J.; Mar, W.; Klein, M. L. *J. Chem. Soc., Faraday Trans.* **1991**, *87*, 2031.

(18) van der Ploeg, P.; Berendsen, H. J. C. *J. Chem. Phys.* **1982**, *76*, 3271.

(19) Cardini, G.; Bareman, J. P.; Klein, M. L. *Chem. Phys. Lett.* **1988**, *145*, 493.

(20) Bareman, J. P.; Cardini, G.; Klein, M. L. *Phys. Rev. Lett.* **1988**, *60*, 2152.

(21) Harris, J.; Rice, S. A. *J. Chem. Phys.* **1988**, *89*, 5898.

(22) Moller, M. A.; Tildesley, D. J.; Kim, K. S.; Quirke, N. *J. Chem. Phys.* **1991**, *94*, 8390.

(23) Mann, J. A.; Tjatjopoulos, G. J.; Azzam, M.-O. J.; Boggs, K. E.; Robinson, K. M.; Sanders, J. N. *Thin Solid Films* **1978**, *152*, 29.

(24) Laibinis, P. E.; Whitesides, G. M.; Allara, D. L.; Tao, Y.-T.; Parikh, A. N.; Nuzzo, R. G. *J. Am. Chem. Soc.* **1991**, *113*, 7152. Bain, C. D.; Biebuyck, H. A.; Whitesides, G. M. *Langmuir* **1989**, *5*, 723. Nuzzo, R. G.; Zegarski, B. R.; Dubois, L. H. *J. Am. Chem. Soc.* **1987**, *109*, 733. Nuzzo, R. G.; Fusco, F. A.; Allara, D. L. *J. Am. Chem. Soc.* **1987**, *109*, 2358.

(25) Nuzzo, R. G.; Dubois, L. H.; Allara, D. L. *J. Am. Chem. Soc.* **1990**, *112*, 558.

(26) Li, Y.; Huang, J.; McIver, R. T., Jr.; Hemminger, J. C. *J. Am. Chem. Soc.* **1992**, *114*, 2428.

electrochemistry,<sup>27</sup> and Raman spectroscopy.<sup>28</sup> The bonding of the thiolate group to the gold surface is very strong (homolytic bond strength is  $\sim 44 \text{ kcal/mol}$ <sup>29</sup>). However, the exact nature of this bonding has never been addressed.

Electron diffraction studies (both high<sup>30</sup> and low energy<sup>31</sup>) of monolayers of alkanethiolates on Au(111) surface show that the symmetry of sulfur atoms is hexagonal with an S-S spacing of  $4.97 \text{ \AA}$  and calculated area *per* molecule of  $21.4 \text{ \AA}^2$ . Helium diffraction<sup>32</sup> and atomic force microscopy (AFM)<sup>33</sup> studies confirmed that the structure formed by docosanethiol on Au(111) is commensurate with the underlying gold lattice and is a simple  $(\sqrt{3} \times \sqrt{3})R30^\circ$  overlayer. Hence, the S-S spacing corresponds to the second-nearest-neighbor distance on Au(111). Scanning tunneling microscopy (STM) studies by Porter *et al.* suggested the same structure.<sup>34</sup> However, recently, Bard *et al.* found that thiolate monolayers, even where the  $\omega$ -substituent size should not allow such a packing, still showed the  $(\sqrt{3} \times \sqrt{3})R30^\circ$  structure, thus suggesting that the previous studies may have been of perturbed gold electronic distribution.<sup>35,36</sup> For a docosanethiolate monolayer on Au(100) surface, the symmetry of the chemisorbed thiolate groups is a simple square lattice with an S-S spacing of  $4.54 \text{ \AA}$ .<sup>30</sup> Note that both the square lattice symmetry and the S-S spacing are not commensurate with the intralayer close-packing arrangement of methylene groups favored by their vdW interactions.<sup>11</sup> Interestingly enough, Scoles *et al.*, using helium diffraction, did not detect a square lattice symmetry for the surface methyl groups in a monolayer of docosanethiolate on Au(100).<sup>37</sup>

LEED–Auger studies of  $\text{CH}_3\text{S}$  on Ag(111)<sup>38,39</sup> suggest an S-S distance of  $4.41 \text{ \AA}$  (epitaxial structure of  $(\sqrt{7} \times \sqrt{7})R10.9^\circ$ ). More recently, Harris *et al.* observed that dimethyl disulfide dissociatively chemisorbs on Ag(111). Their studies confirmed both the above structure and S-S distance. However, for the Ag(100) there were a number of coverage schemes suggested with a variety of S-S distances.<sup>38</sup>

In this paper we report the first *ab initio* geometry optimization of HS and  $\text{CH}_3\text{S}$  on cluster models of Au(111), Au(100), Ag(111), and Ag(100) surfaces at the RECP Hartree–Fock + electron correlation (MBPT2) level of theory. Thus, we provide the missing structural information concerning the chemisorption of thiols on gold and silver surfaces. We further discuss the character of sulfur–metal bonding on the four surfaces concerned. Also presented are the force field parameters needed for molecular mechanics and dynamics simulations of these organic assemblies on these surfaces. We present molecular mechanics (MM) energy minimization of full monolayers of both  $\text{CH}_3\text{S}$  and  $\text{C}_{16}\text{H}_{33}\text{S}$  on Au(111) surfaces, using a modified MM2 force field incorporating the chemisorption parameters. Finally we rationalize the difference between the coverage schemes on Au(111) and Ag(111).

(27) Widrig, C. A.; Chung, C.; Porter, M. D. *J. Electroanal. Chem.* **1991**, *310*, 335.

(28) Bryant, M. A.; Pemberton, J. E. *J. Am. Chem. Soc.* **1991**, *113*, 3629, 8284.

(29) Dubois, L. H.; Nuzzo, R. G. *Annu. Rev. Phys. Chem.* **1992**, *43*, 437.

(30) Strong, L.; Whitesides, G. M. *Langmuir* **1988**, *4*, 546. Chidsey, C. E. D.; Loiacono, D. N. *Langmuir* **1990**, *6*, 709.

(31) Dubois, L. H.; Zegarski, B. R.; Nuzzo, R. G. *J. Chem. Phys.* **1993**, *98*, 678.

(32) Chidsey, C. E. D.; Liu, G.-Y.; Rowntree, P.; Scoles, G. *J. Chem. Phys.* **1989**, *91*, 4421.

(33) Alves, C. A.; Smith, E. L.; Porter, M. D. *J. Am. Chem. Soc.* **1992**, *114*, 1222.

(34) Widrig, C. A.; Alves, C. A.; Porter, M. D. *J. Am. Chem. Soc.* **1991**, *113*, 2805.

(35) Kim, Y.-T.; McCarley, R. L.; Bard, A. J. *J. Phys. Chem.* **1992**, *96*, 7416.

(36) For a critical review on STM see: Frommer, J. *Angew. Chem., Int. Ed. Engl.* **1992**, *31*, 1298.

(37) Camillone, N.; Chidsey, C. E. D.; Liu, G.-Y.; Scoles, G. *J. Chem. Phys.*, in press.

(38) Rovida, G.; Pratesi, F. *Surf. Sci.* **1981**, *104*, 609.

(39) Schwaha, K.; Spencer, N. D.; Lambert, R. M. *Surf. Sci.* **1979**, *81*, 273.

### Ab Initio Calculations

All of the electronic structure calculations presented here are *ab initio* RECP Hartree-Fock + correlation with second-order perturbation theory (MBPT2). We employ the model potential ECP method of Huzinaga *et al.*<sup>40</sup> because this method preserves the nodal structure of the metal atom valence orbitals. We have employed several models of the gold and silver surfaces for the purpose of describing SH and SCH<sub>3</sub> chemisorption. In all our cluster models the orbital occupancy was chosen according to the Stockholm prepared cluster rules.<sup>41</sup> The positions of the metal atoms in the cluster models were held fixed with a nearest-neighbor distance of 2.88 Å for gold and 2.89 Å for silver taken from the bulk. The gold and silver atoms employed in this work are either 11 electron RECP atoms or model atomic potential representations (MAPs).<sup>42</sup> In the 11 electron RECP approximation for Ag or Au atoms the electron density up to and including the 4p (for silver) and 5p (for gold) electron density was replaced by a relativistic effective core potential. The RECP method thus treats explicitly the ten d electrons and the valence s electrons as fully quantum mechanical electrons. The parameters of the RECP were determined by fitting to the orbital shapes and energies of the 4d and 5s Ag atomic orbitals and 5d and 6s Au atomic orbitals obtained from relativistic Hartree-Fock calculations. These Hartree-Fock calculations include the Darwin and mass-velocity relativistic corrections according to the prescription given by Almlöf *et al.*<sup>43</sup> We neglect the spin-orbit coupling. The model atomic potential representations (MAPs) are electrostatic operators that are included in the model Hamiltonian to represent metal atoms that are more distant from the chemisorption site. These model atomic potentials, described elsewhere,<sup>44</sup> have been used successfully in similar calculations of the chemisorption of atomic sulfur on the Pd(111) surface.<sup>45</sup>

Our RECP parameters and basis sets for gold and silver are available from the authors upon request. The projection operator or "killing operator"<sup>46</sup> for gold and silver employed in this work is described by the basis set of Gropen<sup>47</sup> and Hyla-Krispin,<sup>48</sup> respectively. The sulfur and hydrogen basis sets employed in this work were the DZ and DZP basis sets. The valence space of atomic gold contains the 5d and 6s electron density, and so the RECP atom has no p-type basis functions. For binding studies, however, the RECP basis set is supplemented with p-functions. We optimized the exponent of an uncontracted p-type Gaussian for the Ag<sub>12</sub>/Au<sub>12</sub> SH model systems at the Hartree-Fock level. We observed that this set of p-functions made significant contributions to the surface-sulfur bond and to the orbitals involving primarily the metal atoms (in the A<sub>2</sub> space of C<sub>3v</sub>). The calculations were performed on an IBM RS/6000 530 machine and the Cray-2 at the National Center for Supercomputing Applications with the NCSA-DISCO program.<sup>49</sup>

Our past experience with applications of this kind is encouraging. These techniques have predicted vibrational spectra for polyatomic molecules chemisorbed on metal surfaces that agree very well with HREEL data.<sup>44</sup> In calculations of atomic oxygen and sulfur chemisorption on Pd(111), PdX distances agree very well with values from LEED determinations.<sup>45</sup> The accuracy of our results for acetylene on Pd(111) appears to be similar to that obtained by Simandiras *et al.*<sup>46</sup> for free

(40) Huzinaga, S.; Klubokowski, M.; Sakai, Y. *J. Phys. Chem.* 1984, 88, 4880. Andzelm, J.; Huzinaga, S.; Klubokowski, M.; Radzio, E. *Mol. Phys.* 1984, 52, 1495. Huzinaga, S.; Seijo, L.; Barandiaran, Z.; Klubokowski, M. *J. Chem. Phys.* 1987, 86, 2132. Bonifacic, V.; Huzinaga, S. *J. Chem. Phys.* 1974, 60, 2779.

(41) Panas, I.; Schule, J.; Siegbahn, P. E. M.; Wahlgren, U. *Chem. Phys. Lett.* 1988, 149, 26.

(42) Sellers, H. L. *Chem. Phys. Lett.* 1991, 178, 351. Notice that one might debate whether the MAPs should be counted as a part of the cluster. We feel they should. These MAPs are exactly what one gets when one treats atoms classically (rather than quantum mechanically). What one gets with our MAPs is the Coulombic interaction between the quantum mechanical electrons and the MAP atoms. What one does not get is the exchange potential which should be very small since these MAPs represent "distant" metal atoms.

(43) Almlöf, J.; Faegri, K., Jr.; Grelland, H. H. *Chem. Phys. Lett.* 1986, 114, 53.

(44) Sellers, H. L. *J. Phys. Chem.* 1990, 94, 8329.

(45) Sellers, H. L. *Chem. Phys. Lett.* 1990, 170, 5.

(46) Simandiras, E. D.; Rice, J. E.; Lee, T. J.; Amos, R. D.; Handy, N. C. *J. Chem. Phys.* 1988, 88, 3187.

(47) Gropen, O. J. *Comput. Chem.* 1987, 8, 982.

(48) Hyla-Krispin, I.; Demuyncck, J.; Strich, A.; Bénard, M. *J. Chem. Phys.* 1981, 75, 3954.

(49) NCSA-DISCO is a direct SCF and second-order perturbation theory and graphics program under development by H. Sellers. It is based on the DISCO program by Almlöf, J.; Faegri, K., Jr.; Feyereisen, M.; Korsell, K.

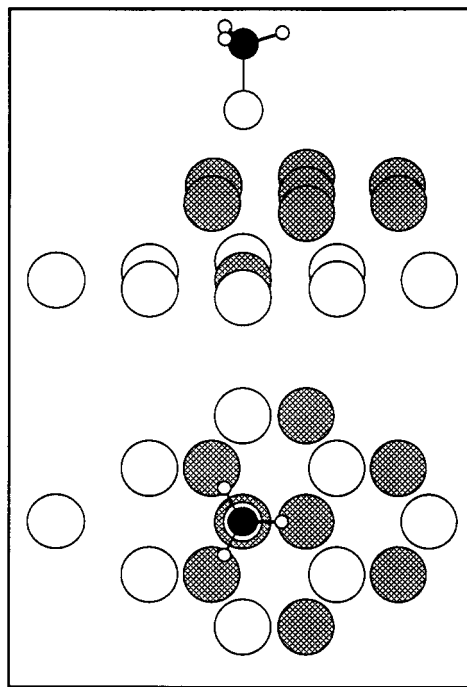


Figure 2. Two views of SCH<sub>3</sub> on the 16-atom model of the (111) surface. The waffle-shaded atoms are 11-electron RECP atoms.

acetylene, namely, that at the Hartree-Fock + MBPT2 level of theory with the DZP basis set, one can expect frequencies to be accurate to about 2%.

Figure 2 shows SCH<sub>3</sub> chemisorbed at the hollow site of a 16-atom cluster model of the (111) surface. We initially optimized the structures of the adsorbates on smaller cluster models of the surfaces and then refined those structures on this larger cluster model. As shown in Figure 2, we employ an atom with quantum mechanical electrons directly below the hollow binding site. The other eight atoms in the second layer are model atomic potential (MAP) atoms.

Figure 3 shows SCH<sub>3</sub> chemisorbed at the hollow site of a 29-atom cluster model of the Au(100) surface. As in our (111) surface calculations, the structures of the adsorbates were optimized on smaller clusters and refined on this larger cluster model of the (100) surface. The four waffle-shaded atoms in the top layer and the one striped atom of the second layer (directly below the 4-fold hollow site) are 11-electron RECP atoms. The atoms of the top layer with checkerboard filling and the open atoms of the second layer are model atomic potential atoms.<sup>42</sup>

### Results and Discussion

**Bonding Schemes.** The structures of SH in the on-top position for the 16-atom cluster models of both Au(111) and Ag(111) surfaces were optimized at the RECP Hartree-Fock + MBPT2 level. These were energy maxima; thus, moving either toward the hollow sites or the bridging sites was downhill in energy. The SH fragment, therefore, was allowed to move off the on-top site and seek its true optimal position and adsorbate geometry for each cluster model. In both cases, the hollow site was more stable (by 6.03 kcal/mol on Au and 3.30 kcal/mol on Ag), and the bend angles indicate a change from sp<sup>3</sup> to sp hybridization for S. Similar sets of calculations on (100) cluster models again found the hollow sites to be energetically preferred (by 5.50 kcal/mol for SH on Au and 5.00 kcal/mol on Ag). Similarly, SCH<sub>3</sub> had a definite preference for hollow sites.<sup>50</sup>

Table I contains geometric information for both the on-top and hollow-site-optimized structures on these surfaces. Unfortunately, there does not appear to be an experimental determination of these structural parameters with which we can compare.

(50) We do not have the energy difference between on-top and hollow site for the SCH<sub>3</sub>, since they were done on different clusters. The on-top position was an energy maximum (i.e., moving in any direction from an on-top site position lowered the energy). The hollow site position was an energy minimum; thus, a definite preference is shown.

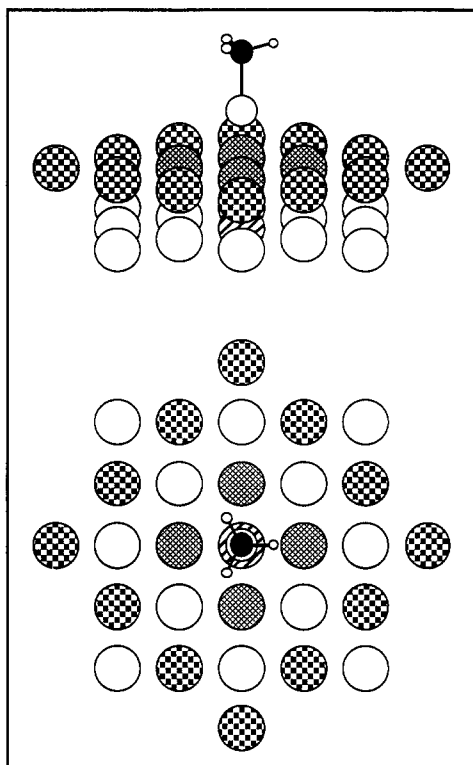


**Figure 3.** Two views of the 29-atom cluster model of the (100) surface. The waffle-shaded atoms and the striped atom in the second layer are 11-electron RECP atoms. The checkered and white atoms are MAP atoms.

**Table I.** Geometry of Optimized Structures on Different Cluster Models

	M-S, <sup>a</sup> Å	M-S-H <sup>b</sup> , deg	S-H, Å
On-Top Sites			
Au(111)	2.715	102	1.393
Ag(111)	2.708	110	1.370
Au(100)	2.153	104	1.380
Ag(100)	2.381	103	1.376
Hollow Sites			
Au(111)	1.978	180	1.353
Ag(111)	2.337	180	1.396
Au(100)	2.038	180	1.372
Ag(100)	2.249	180	1.380
	M-S, <sup>a</sup> Å	M-S-CH <sub>3</sub> , <sup>b</sup> deg	S-CH <sub>3</sub> , Å
On-Top Sites			
Au(111)	2.390	108	1.902
Ag(111)	2.646	105	1.946
Hollow Sites			
Au(111)	1.905	180	1.826
Ag(111)	2.332	180	1.973
Au(100)	2.011	180	1.936
Ag(100)	1.923	180	1.955

<sup>a</sup> The M-S distance is the distance of the sulfur atom from the plane of the surface metal atoms. <sup>b</sup> The angle between the S-R bond (R = H, CH<sub>3</sub>) and the perpendicular from the sulfur to the plane of the surface metal atoms.

However, other metal-sulfur distances are in the same general range, for example, the Pd-S distance on the Pd(111) plane is measured to be 2.22 Å.<sup>51</sup>

Clearly, the top site bonding is different from that in hollow sites. It also appears that (111) surfaces have different bonding than (100) surfaces even for on-top sites. This probably is due

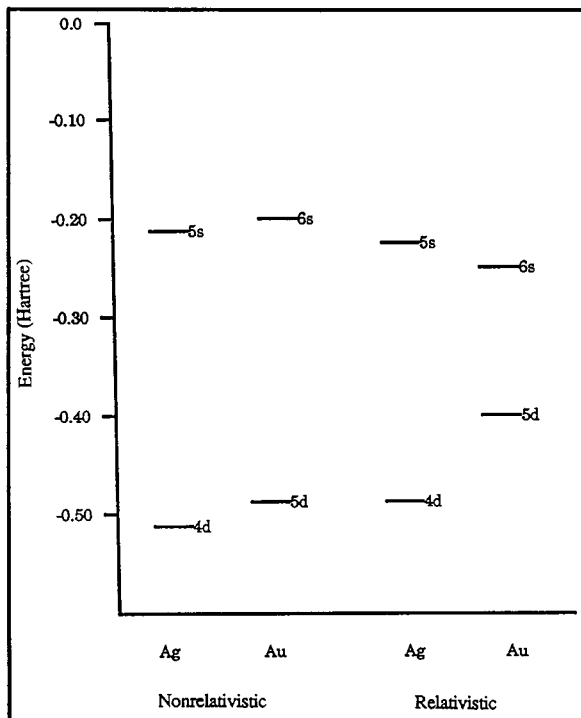


**Figure 4.** Relativistic and nonrelativistic valence space energy levels for atomic silver and gold.

to the number of nearest neighbors and their distance. It also is noticed that the gold surfaces bind S somewhat differently than the silver surfaces do. For metals that have essentially identical interatomic packing arrangements and distances, and that both have d<sup>10</sup>s<sup>1</sup> valence shells, this might seem surprising. However, the first two ionization potentials for Ag are a couple of electron volts lower than those for Au, and relativistic effects are said to "shrink the s-space" of the third-row transition metals more than the second. It is also observed that the Au-Cl bond distance in AuCl<sub>2</sub><sup>-</sup> and the Au-H bond distance in AuH are shorter than for the analogous silver species. Moreover, these metals clearly react differently with elemental sulfur and hydrogen sulfide.

Furthermore, the spread in energies of the valence atomic orbitals, (5s, 4d, 5p) for Ag and (6s, 5d, 6p) for Au, is larger for Ag (Figure 4), and the valence orbitals of atomic silver are significantly more diffuse than those of Au. These atomic orbital differences will result in somewhat different hybridization tendencies for these metals and also in electron clouds that extend higher above the metal surface for Ag. The diffuseness of these orbitals will also strongly influence the degree to which S can penetrate into the hollow sites. Thus, the Ag(100) sites may provide better fits than Ag(111), while for Au, the closer internuclear spacing of (111) may be a better fit. The differences in structure observed for these chemisorptions are quite consistent with the observation that the chemistry of these metals, while similar, shows many significant differences. SCH<sub>3</sub> seems to bind somewhat more tightly than SH in all cases. On Ag(100), the "bond" shortens by 0.3 Å. The SH vs SCH<sub>3</sub> distinction may be related to the availability of p-orbitals in CH<sub>3</sub> that are not available (high energy) with H.

The bonding of the sulfur atom to these metal surfaces involves several metal atoms of the cluster and cannot be interpreted in terms of localized bonds to individual metal atoms. Figure 5-9 show the complex shapes of some of the MOs involved. For on-top sites, the bonding between the surface and sulfur is primarily σ in character, with a small π-contribution, and is concentrated upon a single metal atom. The involvement of other cluster atoms is slight. The sulfur appears to be sp<sup>3</sup> hybridized,



**Figure 5.** The  $\sigma$ -bonding orbital of  $\text{SCH}_3$  to the  $\text{Ag}(111)$  surface in the on-top position.

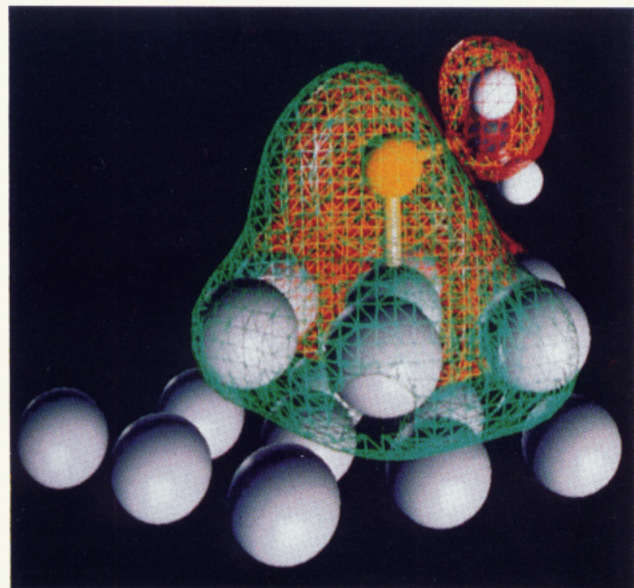


**Figure 6.** The  $\pi$ -bonding orbital of  $\text{SCH}_3$  to the  $\text{Ag}(111)$  surface in the on-top position.

and the bond is quite polar ( $\sim 0.7\text{e}$  in all cases).<sup>52</sup> The  $\sigma$ -bonding is accomplished primarily by the sulfur p-orbitals and the metal 5s/6s-orbitals, with significant contributions from the metal p- and d-orbitals. The p-functions perpendicular to the surface from the neighboring metal atoms also contribute to the  $\pi$ -bonding orbitals. Figures 5 and 6 show isocontours (red net for  $\psi = +0.01$ ; blue net for  $\psi = -0.01$ ) for two of the higher-lying bonding orbitals for  $\text{SCH}_3$  chemisorbed to the  $\text{Ag}(111)$  surface at the on-top position.<sup>53</sup> We remind the readers that a  $\pi$ -orbital is defined as

(52) Charges were obtained from fits of dipole moments as well as the traditional Mulliken population analysis.

(53) Close inspection of the MOs of the bare substrate does not show any significant polarization in any direction. The character of the MOs given in Figures 5–9, therefore, is determined mostly by the symmetry of the adsorbate and influenced very little by the asymmetry of the cluster model.



**Figure 7.** A front-top view of the  $\sigma$ -bonding orbital between the  $\text{SCH}_3$  species and the  $\text{Ag}(111)$  surface in the hollow site position.

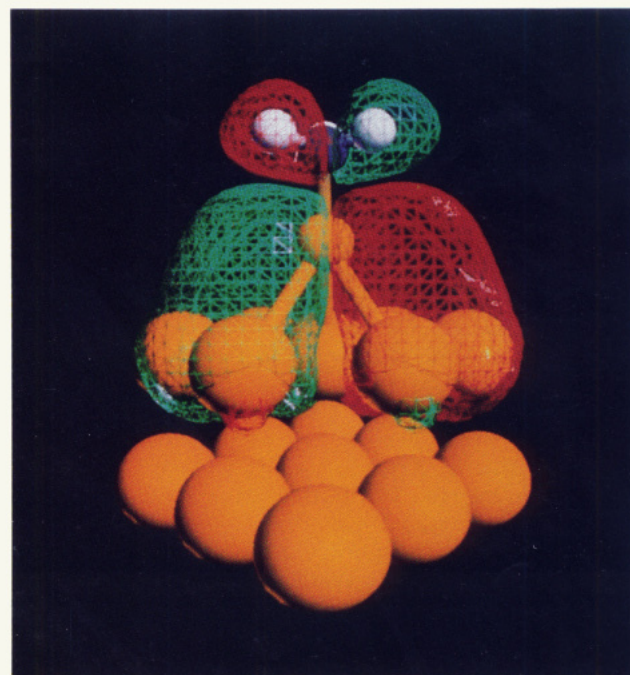


**Figure 8.** A front view of the  $\pi$ -bonding orbital between the  $\text{SCH}_3$  species and the  $\text{Ag}(111)$  surface in the hollow site position.

one that has a single nodal plane containing the bond axis. Here, each  $\pi$ -lobe involves three Ag atoms and s, p, and d basis functions from those atoms. The higher-lying  $\sigma$ - and  $\pi$ -orbitals are actually antibonding with respect to the S– $\text{CH}_3$  bond, which probably accounts for the lengthening of this bond upon chemisorption. Very similar bonding schemes for top-site positions are present between  $\text{SCH}_3$  and the  $\text{Au}(111)$  surface, and between SH and these surfaces.

The bonding scheme for hollow sites also has both  $\sigma$ - and  $\pi$ -character; however, here, there is more  $\pi$ -bonding, and the

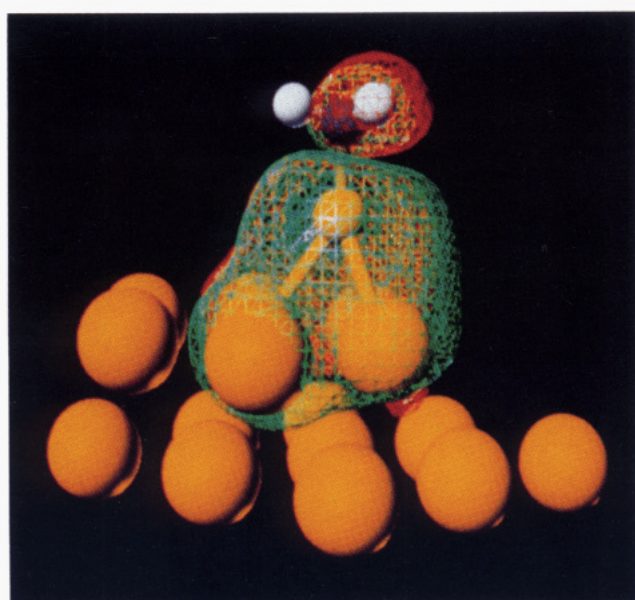


**Figure 9.** A front view of the  $\pi$ -bonding orbital between the  $\text{SCH}_3$  species and the  $\text{Au}(111)$  surface in the hollow site position.

second-layer atom immediately below the hollow site also contributes significantly. Figures 7 and 8 show high-lying  $\sigma$ - and  $\pi$ -bonding orbitals between the  $\text{SCH}_3$  species and the  $\text{Ag}(111)$  surface. The “tripod” is there to emphasize the 3-fold symmetry of the hollow site. The nodal plane is clearly observed in Figure 8. Again, this  $\pi$ -orbital is antibonding with respect to the  $\text{S}-\text{C}$  bond (Figure 8). A close inspection of Figures 6 and 8 reveals that the  $\pi$ -orbital for the hollow site extends over fewer Ag atoms than was the case for the on-top site. The small tails of opposite color (i.e., phase), visible below the large  $\pi$ -lobes in Figure 8, serve to emphasize that metal p-orbitals perpendicular to the surface, and thus perpendicular to the p-orbital of the sulfurs, and metal s-orbitals are involved, rather than those metal p-orbitals parallel to the sulfur p-orbitals, as is the case for classic organic  $\pi$ -bonds. No second-layer atoms contribute to the  $\pi$ -bonding scheme between the sulfur and the surface.

There is some d-orbital participation from the metal, but it is minor. Polarization functions on S also play a very minor role. The hybridization of the sulfur in this case is sp. This hybridization is necessary for sulfur p-orbitals that are parallel to the surface, and thus permits the strong  $\pi$ -bonding with the silver s- and out-of-plane p-orbitals. This is a classic case of  $\pi$ -back-bonding resulting in a sulfur charge of only  $\sim 0.4e$ ,<sup>52</sup> whereas the analogous charge for chemisorption at the on-top site is  $\sim 0.7e$ . Thus, while the bonding in the on-top site is rather *ionic* in nature, that in the hollow site is more *covalent*. Again, very similar bonding schemes were observed for the SH case, and for  $\text{Au}(111)$  hollow-site bonding. Figure 9 shows the  $\pi$ -bonding scheme in the case of  $\text{Au}(111)$ . Note that while at first glance Figures 8 and 9 may look the same, in fact, a close examination shows that the orbital is more disperse in the case of  $\text{Ag}(111)$ .

In general, the bonding schemes on the (100) surfaces are much the same (Table I). The on-top sites of the (100) surfaces are also energy maxima for the SH adsorbate. The S-H adsorbate sits higher above the surface in the silver case, both at the on-top and the hollow sites. On the other hand, the S-CH<sub>3</sub> adsorbate is closer to the surface at the Ag(100) hollow site. Clearly, the difference between the silver and the gold is less pronounced for the (100) surfaces. Similar to the case of the (111) surfaces, as the adsorbates move from the on-top site to the hollow site, the hybridization of the sulfur atom changes from sp<sup>3</sup> to sp, and the  $\pi$ -back-bonding results in a less ionic bond ( $q_S \sim 0.4e$ ).

**Table II.** Structure and Force Constants for the  $\text{Au}/\text{Ag}(111)-\text{SX}$  Systems, Where X = H, CH<sub>3</sub><sup>a</sup>

coordinate	equilibrium value		force constant	
	Au	Ag	Au	Ag
SH				
S-H distance	1.353	1.396	3.648	3.076
surface-S distance	1.978	2.337	0.984	0.637
$h^b-\text{S}-\text{H}$ angle	180.0	180.0	0.840	0.210
$\text{Au}-h-\text{S}$ angle	90.0		0.492	
			-7.857 <sup>c</sup>	
			1356 <sup>d</sup>	
slide <sup>e</sup>		0.0		0.091
$\text{SCH}_3$ (S sp) <sup>f</sup>				
S-CH <sub>3</sub> distance	1.826	1.973	3.000	2.185
surface-S distance	1.905	2.332	0.695	0.179
$h^b-\text{S}-\text{CH}_3$ angle	180.0	180.0	0.020	0.271
$\text{Au}-h-\text{S}$ angle	90.0		1.761	
slide		0.0		0.110
qs <sup>g</sup>	-0.21			
$\text{SCH}_3$ (S sp <sup>3</sup> ) <sup>f</sup>				
S-CH <sub>3</sub> distance	1.817		3.020	
surface-S distance	1.936		0.667	
$h-\text{S}-\text{CH}_3$ angle	104.0		0.322	
slide	0.27		0.291	
qs	-0.39			

<sup>a</sup> Distances are in Å, angles are in deg, stretching force constants are in mdyn Å<sup>-1</sup>, and angle bending force constants are in mdyn Å rad<sup>-2</sup>. We estimate that force constants are accurate to within 2%. <sup>b</sup> h denotes the hollow site. <sup>c</sup> Cubic force constant (energy derivative form) in mdyn Å rad<sup>-3</sup>. <sup>d</sup> Quadratic force constant (energy derivative form) in mdyn Å radian<sup>-4</sup>. <sup>e</sup> Slide is the coordinate for the motion of the whole adsorbate parallel to the surface and defined as the distance of the S atom from a surface normal drawn through the center of the hollow site. <sup>f</sup> The subheadings  $\text{SCH}_3$  (s sp) and  $\text{SCH}_3$  (S sp<sup>3</sup>) refer to the surface-S-C angles of 180° and 104°, respectively. <sup>g</sup> qs is the charge in units of number of electrons. (-1 represents a full electron transfer from the gold cluster to the sulfur atom.)

Before getting into a detailed discussion on force constants, the question of relativistic corrections has to be addressed. It has long been known that the effect of the Darwin and mass–velocity relativistic correction tends to lower the energies of atomic s- and p-orbitals while raising the energy of the d-orbitals. The effects can also be seen in Figure 4, which represents the relativistic and nonrelativistic valence orbital energies of silver and gold. These relativistic orbital energies were taken from our relativistic Hartree–Fock calculations and are reproduced by our RECP basis sets for silver and gold. The effect of the relativistic corrections is such that the gold 6s orbital is lower in energy than the relativistic silver 5s. One can expect that the spatial extent of the relativistic silver 5s orbital is greater than the 6s of gold, and in fact, this can also be seen in the contraction coefficients of these orbitals. One also sees that the opposite is true in the case of the metal valence d-orbitals. In terms of silver and gold metal surfaces, this means that the electron density making up the s-band extends further away from the plane of the nuclei in the case of silver surfaces relative to gold. Furthermore, the smaller energy difference between the 5d and 6s orbitals in the case of gold—compared to the difference between the 4d and 5s orbitals in the case of silver—means that it should be easier to hybridize s,d-orbitals on gold.

This relativistic effect very likely is the reason why the adsorbates are generally sitting higher on the silver surfaces than on gold.<sup>54</sup> We stress here that an account of the relativistic effect, which we obtain via the RECPs, is necessary for the correct description of this phenomenon. It is clear from the data in Table II that attempts to model these systems without accounting for the relativistic effects would miss this aspect of these systems.

(54) For the  $\text{Au}(111)$  and  $\text{Ag}(111)$  on-top sites, the distances should be viewed as equivalent by this methodology.

**Table III.** Structure and Force Constants for the Au/Ag(100)-SX Systems, Where X = H, CH<sub>3</sub><sup>a</sup>

coordinate	equilibrium value		force constant	
	Au	Ag	Au	Ag
SH				
S-H distance	1.372	1.380	3.478	3.622
surface-S distance	2.038	2.249	0.760	0.560
<i>h</i> <sup>b</sup> -S-H angle	180.0	180.0	0.123 (t) <sup>c</sup>	0.190
Au- <i>h</i> -S angle	90.0		0.267 (t)	
			0.556 (b)	
slide <sup>d</sup>	0.0		0.010	
SCH <sub>3</sub>				
S-X distance	1.936	1.955	2.443	2.155
surface-S distance	2.011	1.923	0.794	0.702
<i>h</i> -S-X angle	180.0	180.0	0.172	0.285
Au- <i>h</i> -S angle	88.5		265 (t)	
slide <sup>d</sup>	0.0		0.153	

<sup>a</sup> Distances are in Å, angles are in deg, stretching force constants are in mdyn Å<sup>-1</sup>, and angle bending force constants are in mdyn Å rad<sup>-2</sup>. We estimate that force constants are accurate to within 2%. <sup>b</sup> *h* denotes the hollow site. <sup>c</sup> The (t) and (b) indicate that the H atom or CH<sub>3</sub> group was displaced in a direction directly toward (t) or between (b) gold atoms in the force constant calculations. <sup>d</sup> Slide is the coordinate for the motion of the whole adsorbate parallel to the surface and defined as the distance of the S atom from a surface normal drawn through the center of the hollow site.

**Force Constants.** Table II contains the zero force values and the force constants for SH and SCH<sub>3</sub> for the hollow-site cluster models of Au(111) and Ag(111). There are many geometric descriptions of the energy surface that one could choose. For the Au hollow sites, where the S sat well down in the hollow and mobility upon the surface did not seem to be an issue, we chose the perpendicular surface to S distance, the S-H distance, the bend angle around S, and a “leaning angle”. However, for the potential on the silver we felt that a slide coordinate would be preferable to the leaning coordinate, because a generalization of it that would allow the adsorbate more freedom to leave the hollow binding site could be used in MD simulations. The slide coordinate and force constant parameters in Tables II and III are for the motion of the entire adsorbate parallel to the plane of the surface. The coordinate is a distance from a line, that line being a surface normal passing through the center of the hollow binding site. The fact that the slide force constant is positive reflects the fact that the hollow binding sites are energy minima.

We describe the potential for the “leaning” or orientation of the surface-S bond on the (111) surface with the following equation:

$$V(\theta, \phi) = \frac{1}{2!} F\theta^2 + \frac{1}{3!} K\theta^3 \cos(3\phi) + \frac{1}{4!} L\theta^4 \quad (2)$$

The angle  $\theta$  is the angle between the surface-S bond and the surface normal, and  $\phi$  is the angle between the projection on the Au(111) of the surface-S bond and the reference line (see Figure 10). The  $F$ ,  $K$ , and  $L$  parameters (energy derivatives) are given in Table II. The positive direction for  $\theta$  brings the sulfur toward the groove between the two gold atoms. The negative value of  $K$  causes the energy to be lower for a displacement in the positive direction than for the same displacement in the negative direction. Hence, it is the cubic term that breaks the symmetry of the leaning potential. It should be clear that at  $\phi = 60^\circ$ , the potential is the same as when  $\phi = 0^\circ$ , with the exception that the sign of the cubic term is reversed. The symmetry of the hollow binding site requires the sign of the cubic term to reverse every  $60^\circ$  increment in  $\phi$ . The form of the above potential is correct for values of  $\phi$  of  $0^\circ$ ,  $60^\circ$ ,  $120^\circ$ ,  $180^\circ$ ,  $240^\circ$ , and  $300^\circ$ , as required by the symmetry of the hollow binding site. One might improve upon this form by adding a term that is first order in  $\theta$  and has a  $\phi$  dependence such that it is zero when  $\phi = n60^\circ$ , where  $n = 0, 1, 2, 3, \dots$ . This

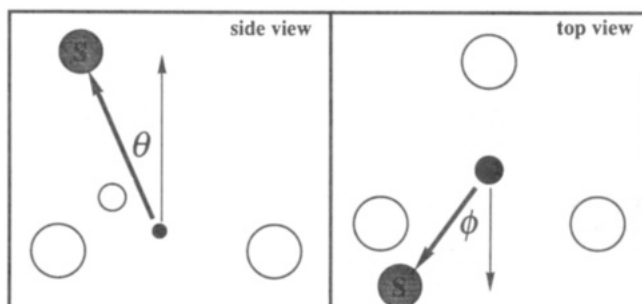


**Figure 10.** The sulfur-surface bond orientation coordinate system on Au(111).

term would describe the shifting of the equilibrium position with respect to  $\theta$  as a function of  $\phi$  and could have the following form:  $A\theta \sin(3\phi)$ . In view of the approximate nature of MD simulations and the other couplings we are neglecting, such as the coupling between the surface-S distance and the angle around the sulfur, it is doubtful that this term would be very important.

Looking first at the S-H results in Table II, we notice that the surface-S stretch is much less stiff than the S-H stretch. The S-H constant is fairly typical for a single bond (bond energy ~80 kcal/mol), and having a smaller value for the surface-to-S stretch is consistent with the observed binding energy (~44 kcal/mol<sup>29</sup>). However, the lack of stiffness for the sulfur-to-surface stretch does not indicate a thermodynamically weak bond. Rather, with the diffuse orbitals involved and the sulfur fitting down into the hollow site, the bond strength is not overly sensitive to small movements of the sulfur. Ag differs from Au in that the S sits higher above the metal surface and can be moved more easily. Thus, the force constant for perpendicular displacement of S is almost 50% smaller, and changing the bend angle around S is four times as easy. This is consistent with the more diffuse s-space of Ag and the greater π-bonding observed for Au.

For SCH<sub>3</sub> on Au(111), the structural parameters and stretching force constants were determined by employing the DZP basis and the MBPT2 method, while keeping the C-H bond distance and S-C-H angle fixed at their equilibrium values, as obtained at the Hartree-Fock level for HSCH<sub>3</sub> in  $C_{3v}$  symmetry. We expect that the freezing of the local CH<sub>3</sub> geometry at these values will have only a minor effect on the computed force constants and geometry parameters of interest. The calculations were performed on smaller clusters and refined on the larger cluster models of the surfaces (Figures 2 and 3).

The linear (sp-like) bend angle around sulfur is somewhat unusual. Since it comes about through moving on sp<sup>3</sup>-like SCH<sub>3</sub> from the on-top site to the hollow site, we tended to consider it as “the minimum energy structure”. However, monolayers of S-(CH<sub>2</sub>)<sub>15</sub>-CH<sub>3</sub> constructed with a linear bond angle around the sulfur would have a direction of tilt opposite that suggested by Nuzzo *et al.*<sup>25</sup> Therefore, we considered the possibility of a second equilibrium position for the bend angle around sulfur.<sup>55</sup> Indeed, SCH<sub>3</sub> in the Au(111) hollow site has two equilibrium values for the bend angle around the sulfur. The 104° bend is the stable one (by 0.41 kcal/mol) and it is much more resistant to deformation (Table II). Intersection of the harmonic curves would estimate the barrier between these minima to come at 123° and have a height of only 2.5 kcal/mol.<sup>56</sup> Thus, it can be expected that an isolated thiolate may easily cross from one of these minima to the other.

Charges of the sulfur (Table II) were estimated from the change in the dipole moment—of the complexes of SCH<sub>3</sub> with the 12-

(55) Before undertaking more extensive calculations, however, we looked for such behavior for S atoms in other molecules. For example, RHF 6-31g\* calculations suggest that while CH<sub>3</sub>-S=C≡CH has only one minimum (bent), CH<sub>3</sub>-S=C≡C-NH<sub>2</sub> also has a second minimum (linear).

(56) The difference of 0.41 kcal/mol is not significant. The barrier may be off by as much as a factor of 2. The whole point is that we have two minima of roughly the same energy with a small barrier between them.

atom gold clusters—with respect to small changes in the surface–S distance. It is assumed that the  $\text{CH}_3$  group is overall neutral and that the positive charge is shared equally by the three Au atoms defining the hollow site.

A close inspection of Table II shows some intriguing differences between the force constants of SH and  $\text{SCH}_3$ . For example, why does the stretching constant for the surface–S distance on Ag decrease by almost  $3/4$  when going from SH to  $\text{SCH}_3$ ? (Note that there is no significant change in height above the surface.) A possible explanation may lie in the  $\pi$ -bonding scheme described above (Figure 7). As the sulfur moves away from the surface, decreasing the  $\pi$ -bonding between the surface and sulfur, rehybridization causes a concomitant decrease in the antibonding character between the sulfur and the methyl group, thus offsetting the energy change. Notice, also, that  $\text{SCH}_3$  sits deeper in the hollow site of Au(111) than does SH, yet it is easier to move the  $\text{SCH}_3$ . Another interesting question is why is it so easy to change the bend angle around S for the  $\text{SCH}_3$  adsorbed on Au(111)? Part of the answer probably lies in the easier mixing of the s-, p-, and d-orbitals (i.e., rehybridization) possible for Au. Finally, why is the leaning potential so much stiffer for  $\text{SCH}_3$  than with SH? Throughout these calculations, we have noticed that the bending force constant around the sulfur is rather sensitive to the perpendicular distance from the sulfur to the surface. This indicates a strong anharmonic coupling between these two vibrational degrees of freedom.

Table III contains force field results for SH and  $\text{SCH}_3$  on the (100) surfaces of gold and silver. The structural parameters for the sulfur–Au(100) surface attachment are very similar in the SH and  $\text{SCH}_3$  systems. Both adsorbates yield a sulfur–surface bond orientation that is (almost) perpendicular to the surface. The  $\text{SCH}_3$  leans  $1.5^\circ$  because the local symmetry of the methyl ( $C_3$ ) and the local symmetry of the metal surface ( $C_4$ ) do not match. In the silver (100) system, this leaning of the  $\text{SCH}_3$  was for all practical purposes negligible (it leans  $0.2^\circ$ ).

All in all, it looks as if  $\text{SCH}_3$  on Ag(111) may be fairly mobile relative to the other systems studied here. The surface–sulfur distance is much larger (by  $0.43\text{ \AA}$ ) than the same distance parameter for the gold surface. This fact, together with the very low perpendicular stretching force constant, indicates that the silver (111) surface quite probably looks relatively flat to the methyl sulfur adsorbate. The slide force constants in Tables II and III are small, and by themselves do not indicate that the adsorbates are mobile, since they are quadratic force constants, and the true hollow site potential could have large—cubic or quadratic—anharmonic terms. However, all the data seen together suggest that the  $\text{SCH}_3$  adsorbate should be much more mobile on the Ag(111) surface than on the Ag(100) surface, or on the Au surfaces. We were not able to perform the electron correlation calculation on a cluster large enough to thoroughly test this hypothesis at this time.

**Chemisorption Scheme.** Electron diffraction experiments with monolayer systems of docosanethiol on single-crystal gold foils with an exposed (111) surface have shown hexagonal packing with an S...S distance of  $4.97\text{ \AA}$ .<sup>30,31</sup> Similarly, the S...S distance on the (100) surface has been reported to be  $4.54\text{ \AA}$ ,<sup>30</sup> exhibiting a base-centered square array. Figure 11 shows the hexagonal arrangement of metal atoms (the open circles) of the (111) surface. This chemisorption scheme based on the electron diffraction results was proposed first by Chidsey *et al.* The black (filled) circles in Figure 11 denote alkanethiolates chemisorbed in hollow sites that are arranged in a hexagonal relationship with respect to each other, as is indicated by the dark lines connecting six of them. Placing the gold atoms at  $5.45$  Bohr ( $2.884\text{ \AA}$ ) from their nearest neighbors (the bulk value for Au) places these hollow sites at a distance of  $4.99\text{ \AA}$  from each other, which is in excellent agreement with the electron diffraction result of  $4.97\text{ \AA}$ . There are two

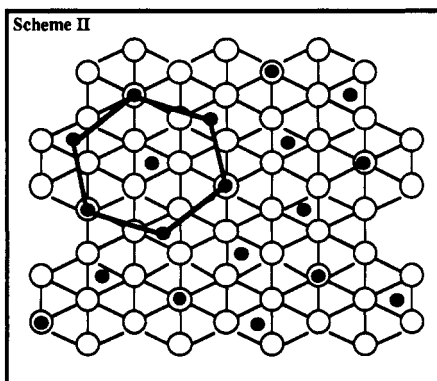
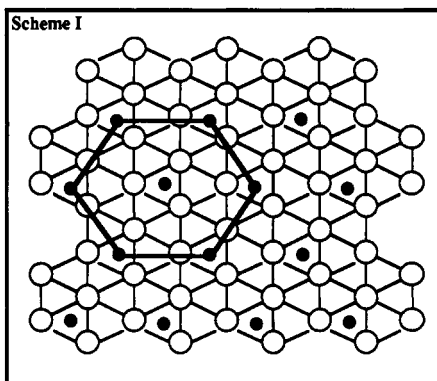


Figure 11. Hexagonal coverage scheme for Au(111) composed of alternating hollow sites.

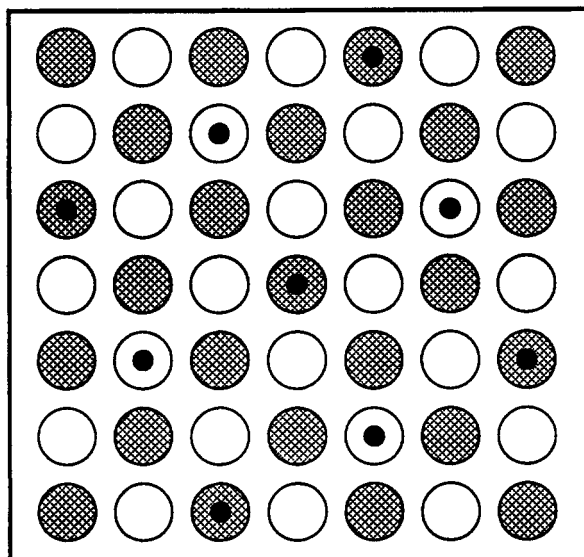


Figure 12. Knight move Au(100) coverage scheme.

types of hollow sites on a (111) surface that we refer to as site A and site B. Site A has a second-layer metal atom directly below the hollow and site B does not. Such an arrangement has the thiolates all in either A sites or B sites. Calculations were done at type A sites only, and found the second-layer atom to be involved strongly in the bonding.

Figure 12 shows top-layer (shaded circles) and second-layer (open circles) atom positions for the (100) surface. The black circles denote chemisorbed alkanethiolate positions. The adsorbate sites alternate between on-top and hollow sites and have the same relationship to each other as the knight move in chess. The “knight move” sites form a base-centered square array with a distance of  $4.56\text{ \AA}$  in very good agreement with the experimental data. Reconciling the different hybridization preferences and

the different natural heights for S atoms above the on-top site vs the hollow site is likely to result in weaker binding for this scheme.

**Molecular Mechanics.** The purpose of this paper has been the calculation of the chemisorption parameters for thiolate groups on gold and silver surfaces using *ab initio* methods. In the previous sections, the results of these calculations were fitted to classical force constants suitable for molecular mechanics and dynamics simulations. Packing and ordering of alkanethiolate chains in their two-dimensional assemblies is determined by the competition between the chemisorption of the thiolate group and the bonded and nonbonded interactions between, as well as within, the hydrocarbon chains. For example, the orientation of the S-C bonds relative to the surface, in a fully packed monolayer, in principle, can be quite different from that of the isolated molecule. Therefore, it is of interest to carry out energy minimizations and molecular dynamics that will incorporate this competition.

We have performed such simulations, using the force field parameters of Table II to augment the MM2 force field.<sup>57</sup> The simulations were performed with POLYGRAF 2.2, using periodic conditions and variable cell dimensions and angles. In each case, the simulation cell contained a single thiolate molecule, the three gold atoms that define the hollow site, a dummy atom that is precisely centered in the hollow site, and a second dummy atom directly underneath the hollow site that is used to define a direction normal to the plane of the gold atoms. (Note that one molecule per unit cell does not explore conformational space in the monolayer. However, we decided to look at this simpler case so that we can better understand the interplay of the binding constant and the intermolecular packing. Full MD simulations at finite temperature with nine molecules per unit cell are in progress.) The gold atoms were not full participants in the molecular minimization. The distance and angles between the three gold atoms were constrained with strong harmonic constraints to values appropriate to Au(111). The van der Waals (vdW) interactions of the gold atoms with C, H, and S were considered to be implicitly contained in the stretching and bending constants of Table II. Partial charges were assigned to the Au and S atoms. A smooth cutoff at 9 Å was used for both Coulombic and vdW terms, and the total potential energy was minimized by using the conjugate gradients method.

Both  $\text{SCH}_3$  and  $\text{SC}_{16}\text{H}_{33}$  monolayers were modeled, first with force constants appropriate for sp, and again for those for  $\text{sp}^3$  sulfur. The minimizations were started with the molecular chains perpendicular to the plane of gold atoms and with a rectilinear cell ( $a = b = 6.0 \text{ \AA}$ ;  $c = 60.0 \text{ \AA}$ ,  $\alpha = \beta = \gamma = 90^\circ$ ). The long third dimension combined with the 9.0 Å cutoff for nonbonded interactions achieves two-dimensional periodicity. During minimization, cell dimensions  $a$  and  $b$  (but not  $c$ ) and angles were allowed to vary and weak constraints were imposed on the dummy atoms to bring the gold atoms to Au(111) conditions. Thus, the chains were permitted to gradually tilt and twist and accommodate their neighbors as the cell was slowly brought to a unit cell consistent with the coverage scheme of Figure 11.

Figure 13 presents “one molecule per unit cell” minimized structures for fully covered monolayers of  $\text{SCH}_3$  moieties on Au(111) surfaces for (a) sp-hybridized sulfur and (b)  $\text{sp}^3$ -hybridized sulfur. In the sp case, the S-C bond is nearly normal to the metal surface; attraction between molecules has not achieved appreciable tilt even though the bending constant around the S atom is very small. MD simulations at 123 K (not shown here) revealed significant tilt fluctuations (up to  $10^\circ$ ). In the  $\text{sp}^3$  case, on the other hand, the S-C bond is almost parallel to the surface. This is the result of the  $104^\circ$  bend angle combined with the slide coordinate that causes the sulfur to “lean” away from the surface



**Figure 13.** A nine-molecule section of a fully-covered  $\text{SCH}_3$  monolayer on Au(111) minimized with a modified MM2 force field including the (a) sp and (b)  $\text{sp}^3$  chemisorption parameters. We have used one molecule per unit cell with periodic boundary conditions and a nonbond cutoff of 9 Å. The gold atoms are shown in light gray having their full van der Waals radii. The sulfur atoms are shown in dark gray and are not drawn to scale.

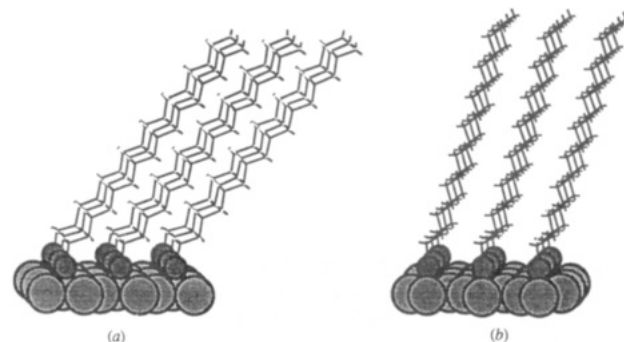


**Figure 14.** Two views of the tilt in a nine-molecule section of a fully-covered  $\text{SC}_{16}\text{H}_{33}$  monolayer on Au(111) minimized with a modified MM2 force field including the sp chemisorption parameters. We have used one molecule per unit cell with periodic boundary conditions and a nonbond cutoff of 9 Å. In a, the tilt in the plane that bisects the  $\text{CH}_2$  groups is shown, while in b, the tilt out of this plane is presented. The gold atoms are shown in light gray having their full van der Waals radii. The sulfur atoms are shown in dark gray and are not drawn to scale.

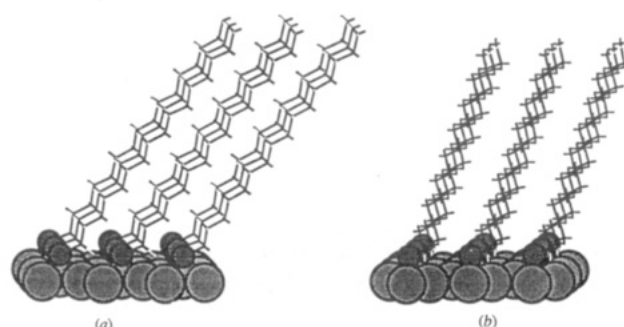


**Figure 15.** Two views of the tilt in a nine-molecule section of a fully-covered  $\text{SC}_{16}\text{H}_{33}$  monolayer on Au(111) minimized with a modified MM2 force field including the  $\text{sp}^3$  chemisorption parameters. We have used one molecule per unit cell with periodic boundary conditions and a nonbond cutoff of 9 Å. In a, the tilt in the plane that bisects the  $\text{CH}_2$  groups is shown, while in b, the tilt out of this plane is presented. The gold atoms are shown in light gray having their full van der Waals radii. The sulfur atoms are shown in dark gray and are not drawn to scale.

normal. There is little distortion from the geometry that a single molecule would adopt in the absence of neighboring adsorbates.

Figures 14 and 15 show optimized packing conformations of a fully covered monolayer of  $\text{SC}_{16}\text{H}_{33}$  on Au(111) surface for sp and  $\text{sp}^3$  chemisorption, respectively. Note that in both cases the chains have an absolute tilt of  $\sim 30^\circ$  from the surface normal, in agreement with both experimental results,<sup>58,59</sup> and previous MM<sup>11</sup> and MD<sup>17</sup> simulations. However, the two optimized packing conformations—based on the sp and  $\text{sp}^3$  chemisorption modes—differ significantly from each other in that they result in different orientations of the terminal  $\text{CH}_3$  group relative to the monolayer surface. Note that the assembly depicted in Figure

(57) Mohamadi, F.; Richards, N. G. J.; Guida, W. C.; Liskamp, R.; Lipton, M.; Caufield, C.; Chang, G.; Hendrickson, T.; Still, C. W. *J. Comput. Chem.* 1990, 11, 440.

(58) Nuzzo, R. G.; Zegarski, B. R.; Dubois, L. H. *J. Am. Chem. Soc.* 1987, 109, 733.

(59) Porter, M. D.; Bright, T. B.; Allara, D. L.; Chidsey, C. E. D. *J. Am. Chem. Soc.* 1987, 109, 3559.

15 has been suggested as the sole possible monolayer structure. Our minimization results show, however, that the molecular mechanics energies of the two structures differ by less than 1 kcal/mol, and thus must be considered identical, for all practical purposes.

### Arguments

Modeling of packing and ordering of complex systems can be approached on different levels of sophistication. The present work represents the first study addressing the role of chemisorption in the balance between the competing forces responsible for the ordering of alkanethiolate monolayers using quantitative tools such as *ab initio* calculations and MM simulations. Detailed MD simulations are in progress and the results will be published in a separate report.

We start with a discussion of the consistency of our *ab initio* and MM results with experimental and simulation studies, with an emphasis on new insights emerging from this work. The most detailed experiments to date were carried out on alkanethiolate monolayers adsorbed on (111) surfaces; therefore, we focus our attention to these systems. First, let us discuss our *ab initio* and MM results on the chemisorption and the resulting ordering in alkanethiolates chemisorbed to Au(111).

A most surprising feature of the present studies is the existence of two stable and energetically competitive hybridizations for the S atom when an isolated  $\text{SCH}_3$  chemisorbs to Au(111). When analyzing data either from experiments or from simulations, most studies make an implicit assumption of an  $\text{sp}^3$  hybridization (a surface–S–C angle near  $109^\circ$ ) of the chemisorbed sulfur atom. Our *ab initio* calculations, on the other hand, indicate that there is another possible hybridization ( $\text{sp}$ , a surface–S–C angle of  $180^\circ$ ) that is nearly as stable.<sup>60</sup> Our MM studies indicate that those two chemisorption minima can lead to monolayers exhibiting similar packing arrangements that are comparable in their ground-state energies. Reevaluation of experimental and simulation data, therefore, may be warranted. For example, most existing FTIR data make the implicit assumption that the entire monolayer consists of molecules having the same bonding to the surface. If, as our study suggests, the two chemisorption modes are similar in their stability, it is quite conceivable that the macroscopic sample may contain both kinds of chemisorption modes to the surface. One possibility may be that the two different modes order in different domains—simultaneously coexisting *homogeneous* clusters, each characterized by a different conformer in their unit cell. The second, and less likely possibility, is that the macroscopic sample is homogeneous, but the unit cell contains molecules in both conformations. This should be rejected, however, since odd-even effects should not be observed (see below). Of course, this possibility still can exist as a part of a system that also contains other unit cells containing only one conformation. The present study was limited to the first, simpler possibility. It is important to emphasize that most spectroscopic probes of monolayers collect the signal over a region of macroscopic size. Hence, if clusters of different conformers coexist in such a region, the measured signal will consist of separate contributions from the different conformers. Thus, interpretation of the signal becomes a more complex, demanding task, and depends on the estimate of the relative population of the different conformers, which may vary with chemisorption protocol and temperature, and exhibit metastability. In the latter case, annealing the monolayer should strongly affect the relative population of the different chemisorption isomers. It is noted that the effectiveness of this annealing should be a function of the chain length, surface roughness, concentration of defects, contamination, and temperature.

(60) Since occupation of neighboring sites is sure to affect the strength of the chemisorption bond, one should not place too much significance on the 0.4 kcal/mol extra stabilization for the  $\text{sp}^3$ -like case.

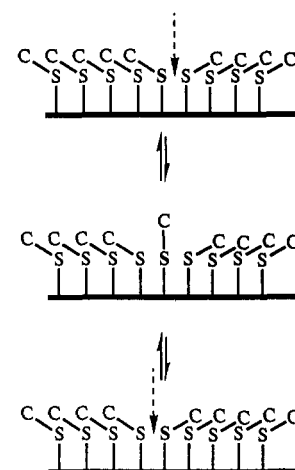


**Figure 16.** A possible scenario for annealing of alkanethiolate monolayers. The hybridization change results in the motion of only one chain. The arrow represents the grain boundary. Notice that after the molecule has moved, the grain boundary moved from the right of to the left of that molecule.

The above discussion pertains to an annealing process where the domains have different chemisorption modes. Another form of annealing is where the domains have the same chemisorption mode, but a different orientation with respect to the substrate lattice. Figure 16 presents a possible scenario for the annealing process, where molecules change clusters simply by moving through an  $\text{sp}$ -hybridized conformer. Our prediction is that the process of changing tilt direction should occur well below the melting point of the monolayer; however, it should be a function of chain length. In the annealing process, molecules move through a grain boundary from one cluster to another, and large clusters grow at the expense of small ones. In fact, recent X-ray data clearly show narrowing of the diffraction peak when monolayers of alkanethiolates on Au(111) were annealed.<sup>61</sup> A development of larger domain size was the apparent result of the heating and cooling process.

We have carried out minimizations of monolayers of methanethiolates on Au(111), modeled by one molecule in a unit cell using both chemisorption potentials. It was found that at 0 K the two structures are very similar in energy. Interesting HREELS studies of this monolayer suggest that the S–C bond is tilted with respect to the surface normal.<sup>62</sup> The authors did not consider the possibility of coexisting conformers, and since they did not provide a quantitative analysis of the tilt angle, it is not possible to relate their experiment and our model in a more quantitative fashion.

There has been a consensus in the literature that alkyl chains in monolayers of alkanethiolates on Au(111) are tilted  $\sim 30^\circ$  with respect to the surface normal. This value has been observed consistently by many groups, for many different thiolates, and using different analytical techniques (e.g., FTIR,<sup>63</sup> electron diffraction,<sup>30,31</sup> X-ray diffraction,<sup>61</sup> etc.).<sup>64</sup> Both of our two optimized structures from MM minimizations of monolayers of  $\text{SC}_{16}\text{H}_{33}$  based on  $\text{sp}$  (Figure 14) and  $\text{sp}^3$  (Figure 15) chemisorption parameters are consistent with this conclusion. However, the orientation of the top methyl surface is quite different in the two resulting surfaces. The bond to the  $\text{CH}_3$  group is oriented almost

(61) Liang, K. S.; Fenter, P.; Eisenberger, P. *Phys. Rev. Lett.*, submitted for publication.

(62) Harris, A. L.; Chidsey, C. E. D.; Levino, N. J.; Loiacono, D. N. *Chem. Phys. Lett.* 1987, 141, 350.

(63) Laibinis, P. E.; Whitesides, G. M.; Allara, D. L.; Tao, Y.-T.; Parikh, A. N.; Nuzzo, R. G. *J. Am. Chem. Soc.* 1991, 113, 7152.

(64) Recent X-ray diffraction studies suggested a tilt angle of  $12 \pm 1^\circ$  along the nearest-neighbor direction (Samant, M. G.; Brown, C. A.; Gordon, J. G., II *Langmuir* 1991, 7, 437). These results clearly are in disagreement with data coming out from a number of groups using different analytical techniques.

normal to the surface in Figure 15, while in Figure 14 it has a large projection onto the surface plane. The difference between the two structures can be traced to the different chemisorption parameters— $sp$  vs  $sp^3$ —and the resulting orientation of the S–C bond. Both optimized structures are assemblies of *all-trans* chains, and thus it is clear that adding an odd number of carbons to the chains of Figures 14 and 15 will alternate the relative orientation of the  $\text{CH}_3\text{—CH}_2$  bond with respect to the surface, while adding an even number of carbons will not. If the macroscopic sample is homogeneous, and consistently prefers one chemisorption mode, this should give rise to an odd-even effect in both wetting and FTIR studies. If odd-even effects are not observed, it may suggest a mixture of conformers with roughly equal abundance of the two. We notice that odd-even effects were not observed in wetting by Laibinis *et al.* for monolayers of alkanethiolates on Au(111),<sup>63</sup> however, Porter *et al.* have detected recently such effects in the wetting of these monolayers.<sup>65</sup> Furthermore, they observe the diminishing of odd-even effects with the increasing alkyl chain length. On the other hand, recently, odd-even effects were observed clearly in SAMs of alcanoic acids on  $\text{Ag}_2\text{O}$ , both in wetting and in FTIR.<sup>66</sup> There, FTIR studies showed that the carboxylate group is attached to the surface with both oxygens, that there is only one chemisorption mode, and that the chains are tilted 15–25° with respect to the surface normal. Porter *et al.* also observed an odd-even effect in wetting—using both water and hexadecane as probing liquids—of alkanethiolate monolayers on Ag(111).<sup>67</sup> Similar effects were clearly observed both for the symmetric and asymmetric methyl vibrations— $\nu_s(\text{CH}_3, \text{FR}_2)$  and  $\nu_a(\text{CH}_3, \text{ip})$ , respectively.<sup>67</sup>

Before getting into more detailed explanations, it is important to note that annealing experiments of alkanethiolate monolayers on Au(111) imply that the chemisorption process yields multi-domain SAMs that are not at their global free energy minimum,<sup>61</sup> and hence support the assumption that chemisorption of alkanethiolates on Au(111) is a kinetically controlled process.<sup>1</sup> Furthermore, these experiments show that the length-scale of domains in the annealed samples is limited by the underlying gold substrate for the short-chain samples, and is much shorter for the long-chain ones. With this information in hand, we assume that since there is no competition between chemisorption and vdW interactions—as is apparent from Figures 14 and 15—the chain length discriminates between the two chemisorption modes. Thus, the ratio between the difference in chemisorption energy and the total energy of monolayer formation should be considered. This ratio decreases with the increasing chain length. Thus, for short alkyl chains, where vdW energy is relatively small, the thiolates may prefer mostly one mode, while for long alkyl chains the two modes coexist with relatively similar concentrations, thus diminishing the odd-even effects.

The observation that the same absolute value of the chain tilt (in a plane that bisects the  $\text{CH}_2$  groups) with respect to the surface normal can give rise to two distinct structures with different projections of the  $\text{CH}_2\text{—CH}_3$  bond onto the surface was made by Nuzzo *et al.* in connection with their FTIR results.<sup>25</sup> They compared FTIR spectra of  $\text{S}(\text{CH}_2)_{16}\text{—CH}_3$  and  $\text{S}(\text{CH}_2)_{17}\text{—CH}_3$  monolayers on Au(111) surfaces. The first exhibited intense asymmetric and weak symmetric methyl C–H stretches, while the second exhibited nearly equal intensities of symmetric and asymmetric C–H stretches. They stated that these observations can be rationalized only for structures picking the  $sp^3$  chemisorption isomers (a surface–S–C bond angle of ~110°). They noted, however, that other absolute tilt values would require "...a severe perturbation of a typical divalent sulfur bond angle (~110°) to accommodate the chain packing." The *ab initio*

(65) Walczak, M. M.; Stole, S. M.; Chau, L. K.; Smith, E. L.; Porter, M. D., private communication.

(66) Tao, Y.-T., preprint.

(67) Walczak, M. W.; Chung, C.; Stole, S. M.; Widrig, C. A.; Porter, M. D. *J. Am. Chem. Soc.* 1991, 113, 2370.

study presented here, on the other hand, shows that the surface–S–C bond angle accommodates two local minima for the chemisorption of an isolated  $\text{SCH}_3$  to Au(111) surface, and in fact the  $sp$  chemisorption mode with the surface–S–C bond angle of 180° is nearly as stable as the  $sp^3$  one. Moreover, our MM minimizations show that chain-packing does not significantly perturb the surface–S–C bond angle in either chemisorption mode, giving rise to two monolayer structures that are close in energy, with chains tilted ~30° to the normal, which have different projections of the  $\text{CH}_2\text{—CH}_3$  bond to the surface. Nuzzo *et al.* interpreted their results, within the first-order analysis, assuming that the contribution to the FTIR signal comes from a single homogeneous region composed of one closely packed chemisorption isomer. However, the results presented in this paper suggest that their data may accommodate an alternative interpretation, i.e., that the FTIR signal includes contributions from both of the two chemisorption isomers packed, for example, in the form of coexisting domains of closely packed chains. It is important to emphasize that according to our suggested interpretation, odd-even effect in wetting and in FTIR spectra would still be observed, provided that the population of the two different chemisorption isomers is significantly different.

SAMs of alkanethiolates on Au(111) and Ag(111) surfaces are very different. Thus, while there has been a consensus on the value of the chain tilt on Au(111), the experimental picture for thiolates on Ag(111) has been considerably less clear. Porter, using our published FTIR spectrum of a SAM of dodecanethiolate ( $\text{SC}_{12}\text{H}_{25}$ , ODT) on Ag(111),<sup>68</sup> calculated a tilt angle of ~7°.<sup>69</sup> In another case, we found that the FTIR spectrum of HUT/Ag(111) (HUT being  $\text{HO}-(\text{CH}_2)_{11}-\text{SH}$ ) is featureless, indicating that the chains in this monolayer are perpendicular to the surface.<sup>70</sup> In a detailed study comparing thiols on gold, silver, and copper, Laibinis *et al.* reported that the tilt angle in monolayers on silver is ~12°.<sup>63</sup> Walczak *et al.* reported a tilt angle of 13°,<sup>65</sup> and recent Raman studies suggested a tilt angle of 15°.<sup>28</sup> This is quite a range of tilt angles, indicating that there may be a correlation between surface details and preparation protocol, and the resulting monolayer structure. Indeed, Fenter *et al.* carried out X-ray studies of thiols on gold and on the most carefully prepared sample of Ag(111) to date.<sup>71</sup> Their most current data show unambiguously that the tilt angle in thiols on silver may be as small as  $3 \pm 1^\circ$ ,<sup>72</sup> and that the assembly of thiolates is commensurate with a compressed, orthorhombically distorted Ag(111) surface.<sup>61</sup> Recently, we have carried out surface plasmon Raman spectroscopy studies of alkanethiolate monolayers on Ag(111), Cu(111), and Au(111) surfaces. The tilt angles estimated from these studies were  $0 \pm 5^\circ$ ,  $5 \pm 5^\circ$ , and  $27 \times 5^\circ$ , respectively.<sup>73</sup> Therefore, for the present discussion, we assume that the tilt angle on Ag(111) is close to zero. We argue that the results of the present *ab initio* study of the chemisorption of thiolates on gold and silver surfaces may help to rationalize the observed experimental differences.

We now think that thiolate chemisorption on these (111) surfaces must adopt one of two coverage schemes. Scheme I is shown in Figure 11. It shows epitaxy to the top layer of metal atoms, resulting in hexagonal packing with an S···S distance of 4.99 Å, and has every other hollow site occupied by an adsorbate. This is the coverage scheme observed on Au(111). Scheme II is emerging as our picture for the epitaxial chemisorption of

(68) Ulman, A. *J. Mater. Educ.* 1989, 11, 205.

(69) Porter, M., private communication.

(70) Ulman, A., unpublished results.

(71) Fenter, P.; Eisenberger, P.; Li, J.; Camillone, N., III; Bernasek, S.; Scoles, G.; Ramanarayanan, T. A.; Liang, K. S. *Langmuir* 1991, 7, 2013. Please note that the assumption in this paper that chemisorption of thiolates on Ag(111) is not commensurate has been changed. See ref 60.

(72) Tilt angles varied from 3° to  $8 \pm 1^\circ$ . The Princeton group concluded from their studies that the tilt angle is *very sensitive* to the protocol of surface and monolayer preparation.

(73) Nemetz, A.; Fischer, T.; Knoll, W.; Ulman, A. *J. Phys. Chem.*, in press.

alkanethiolates on Ag(111) and is described in Figure 11. This scheme exhibits the S···S distance of 4.4 Å, which is almost optimal for the packing of alkyl chains that are almost perpendicular to the surface, and can be described as  $(\sqrt{7} \times \sqrt{7})R10.9^\circ$ . Note that the distance of closest approach of the alkyl chains is 4.24 Å (calculated by MM simulations)<sup>11</sup> and that for any greater distance the chains must tilt to maximize their vdW interactions.<sup>11,74</sup> In fact, a value of 4.24 Å has never been observed experimentally, and the value of 4.45 Å should be used instead. This is the chain···chain distance in orthorhombic polyethylene.<sup>75</sup> Notice that the cross-sectional area of a methylene ( $\text{CH}_2$ ) group is oval in shape with a ratio of ~1.13 between the two axes. Thus, the touching distance in the short axis direction is ~3.9 Å, which results in an area of ~17.5 Å<sup>2</sup>/CH<sub>2</sub>. It can be expected, therefore, that chemisorption of thiolate on Ag(111)—as depicted in Scheme II (Figure 11)—may result in a slightly distorted underlying silver lattice, as, indeed, was observed.<sup>61</sup>

It is true that the distance of 4.4 Å has been observed for monolayers of  $\text{CH}_3\text{-S}/\text{Ag}(111)$ ; however, if chemisorption is the dominating factor in determining the adsorption scheme—as is assumed here, and experimentally found for Au(111) surfaces—it is reasonable to suggest that alkanethiolates will chemisorb on Ag(111) in a similar fashion. This kind of surface overlayer on Ag(111) has been observed experimentally for the chemisorption of sulfur atoms,<sup>39</sup> and of SH groups.<sup>38</sup> Scheme II also results in hexagonal packing. However, here there are two types of occupied sites. Each hexagonal unit has one on-top site and two hollow sites occupied by adsorbates. The selection between these two possibilities (Schemes I and II) will depend, among other things, upon details of the energetics of bonding to the surface.

The coverage, free volume, tilt angles, etc., realized in any self-assembled monolayer results from the often competitive requirements of chain–chain energetics, intrachain energetics, and surface-to-adsorbate binding. It is instructive to consider the tradeoffs that result in the different self-assembled structures observed on *ideal* (i.e., atomically smooth) gold and silver (111) surfaces. Let us first consider the chain–chain energetics. As first suggested by Outka *et al.*,<sup>76</sup> and later discussed in some detail by Ulman *et al.*,<sup>11</sup> only certain combinations of chain–chain separation (i.e., lattice spacing) and tilt angles permit *truly* effective packing of alkyl chains. The most effective packing is a trigonal lattice with spacing near 4.45 Å with a molecular axis oriented normal to the surface. The second most effective has a lattice spacing near 5.0 Å and the molecular axis tilted ~30°, such that the distance between the chains is again 4.45 Å and the fit of bulges into depressions is again perfect. It can be thought of as a ratchet that has “slipped by precisely one notch” (see Figure 14). Thus, the interchain energy preference for Scheme II should not depend on chain length. For lattice spacings intermediate between these two, *all-trans* alkyl chains cannot attain a similarly effective packing, no matter what tilt is adopted, and could, in principle, forfeit a large fraction of the possible favorable vdW interactions.<sup>5</sup> Such lattice spacings should result in significant free volume, disordered chains, random tilt directions, and other defects. Thus, interchain energetics discriminate strongly against all but two spacing/tilt combinations, and mildly favors the more densely packed of the two.

A second consideration is that crowding more molecules per unit surface area will also result in more vdW attraction for the entire system simply because there are more chains involved, unless the attraction per chain is diminished. This can amount to a lot of energy, since Scheme II has 29% more chains per unit area than Scheme I. Crowding more molecules onto a given

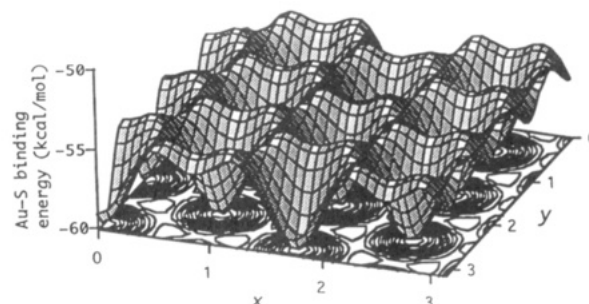


**Figure 17.** A schematic view of the binding energy surface for thiolates on Au(111). Energy minima represent hollow sites.

surface will also be favored by chemisorption potentials that are strong but relatively smooth. If the overall system has a significant favorable change in energy every time another molecule leaves solution and binds to the surface, there will be a large driving force in favor of packing as many adsorbates as possible onto the surface. Thus, both chain–chain interaction and surface-bonding effects favor Scheme II.

Why, then, does chemisorption of thiolates on Au(111) utilize Scheme I? There are two fundamental reasons. First, the above effects are partially offset by the charge–charge repulsions among both S and Au atoms. Sulfur atoms bound to on-top sites (utilized only in Scheme II) have a net charge of ca. -0.7e, where those in the hollow site are ca. -0.4e. Moreover, in Scheme II every seventh gold atom (occupied on-top sites) has a positive charge of ca. +0.7e, while the others are about 0.4e/3, as are all gold atoms in Scheme I.<sup>77</sup> Secondly, and most importantly, chemisorption potentials with significant lateral discrimination could counter the favorable effects of this figure crowding. It is the combination of both lateral discrimination and electrostatic effects that distinguishes the chemisorption of thiolates on Au(111) from that on Ag(111).

Let us discuss how that lateral discrimination arises. Two issues must be considered. The first is how the energy of binding an adsorbate to a surface will vary for different positions on that surface. Figure 17 is a sketch of optimum binding energy of a single thiolate at different x,y coordinates on a (111) surface of either gold or silver. Note that the binding energy is large and negative for all x,y points (~44 kcal/mol<sup>29</sup>). Superimposed on that is a certain regular roughness or undulation indicating site discrimination. The depressions correspond to the most favored binding sites (hollow sites of Figure 11), and the peaks are the least favored sites (on-top positions of Figure 11). Gold differs from silver primarily in the peak-to-valley roughness, 6.0 kcal/mol for Au(111) and only 3.3 kcal/mol for Ag(111). (For other surfaces and/or substrates, we would also see differences in topology, in the spacing between peaks, and in the height of the barriers between favored sites.)

In calculations such as those presented here, a remaining question is the following: *What effect do neighboring adsorbates have on each other?* This is especially important when chemisorption occurs at different sites, resulting in different binding energies and electron densities. Therefore, we decided to address this problem—in part—for SH adsorbates in the knight move coverage scheme on the Au(100) surface (Figure 18).<sup>78</sup> We have performed RECP Hartree–Fock + MBPT2 calculations on the  $\text{Au}_{45}\text{SH}$  and  $\text{Au}_{45}(\text{SH})_5$  systems in an effort to assess the change in binding energy that the surrounding four SH adsorbates in hollow site positions have on the binding of the SH group that

(74) Wunderlich, B. *Macromolecular Physics*; Academic Press: New York, 1973; Vol. 1.

(75) Seto, T.; Hara, T.; Tanaka, K. *Jpn. J. Appl. Phys.* **1968**, *7*, 31.

(76) Outka, D. A.; Stöhr, J.; Rabe, J. P.; Swalen, J. D.; Rotermund, H. H. *Phys. Rev. Lett.* **1987**, *59*, 1321.

(77) One could view this simply as a rationale for weaker chemisorption bond for full coverage.

(78) We decided to study this system for two reasons: (a) It has been studied by Strong and Whitesides,<sup>30</sup> and (b) it has the symmetry that allows such huge calculations to be carried out.

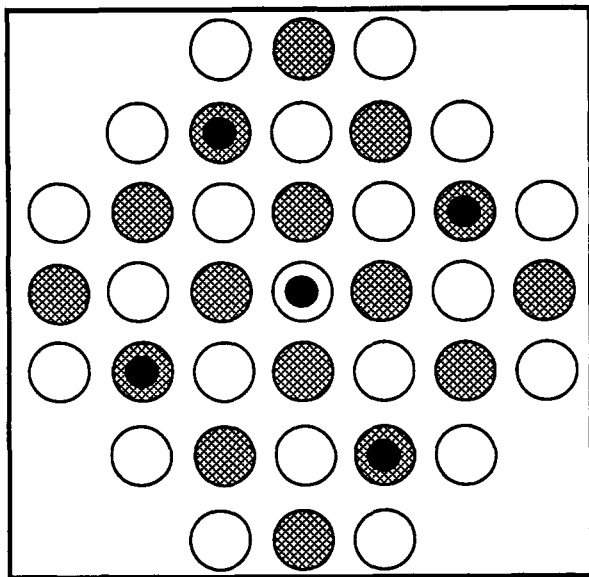
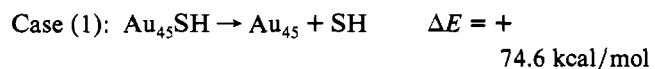
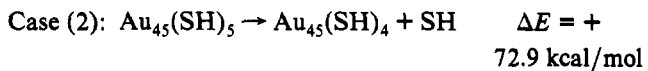


**Figure 18.** Relative positions of the SH groups in the  $\text{Au}_{45}(\text{SH})_5$  system. The top layer atoms (hollow) are 11-electron RECP atoms and the second layer atoms (waffle-shaded) are 1-electron RECP atoms. The black circle represent the sulfur atoms. Notice that the center SH group is at the on-top site and the four surrounding SH groups are at hollow sites.

occupies the on-top position in the knight move scheme.<sup>79</sup> The following binding processes were considered for clusters of 45 gold atoms:



(79) The cluster was similar in structure but larger than that depicted in Figure 3. The top layer atoms are 11-electron RECP atoms and the second layer atoms were 1-electron RECP atoms. There were no MAPs because there were five adsorbates bonding to it, and so there needed to be as many quantum mechanical electrons as possible.



The "dissociated" systems were calculated with the SH displaced along the surface normal to 25 Bohr from the on-top binding site and calculated as the high-spin diradical state. Due to the magnitude of the computational effort involved, no structural optimization at the binding sites was performed. Rather, equilibrium structures from Table I were assumed to apply. This clearly is not a good approximation for the multiple adsorbate cluster, and it is hard to estimate its effect on  $\Delta E$  for case 2. We stress that Hartree-Fock + MBPT2 calculations have a reputation of overestimating binding energies. Therefore, we focus here on the difference between them (1.7 kcal/mol). That the bound adsorbates have a weak inhibitory effect is consistent with ones expectations from simple charge repulsion arguments. However, one might argue that the binding energies are too close for the difference to be meaningful. Wave function and electron density images both provide evidence for significant coaction of adsorbates for case 2. Interestingly enough, we have found that there is a significant amount of electron density between the on-top adsorbate and the four surrounding adsorbates, while there does not seem to be any evidence for any bonding interaction between adsorbates in the hollow sites. To our knowledge, this is the first evidence of adsorbate-adsorbate bonding interaction in a chemisorbed system.

**Acknowledgment.** The authors thank Eastman Kodak Company and the National Center for Supercomputing Applications for support of this work and IBM Corporation for the IBM RS/6000-530 machine on which most of these calculations were performed. H.L.S. thanks Mr. Pierre Dewey La Fontaine, Jr., for his many contributions and dedicates this work to the occasion of his 60th birthday in July 1990. We thank Prof. Michael L. Klein of the University of Pennsylvania and Prof. Giacinto Scoles, Prof. Peter Eisenberg, and Dr. Paul Fenter, all of Princeton University for many discussions.